PCCP

RSC Publishing

PAPER

View Article Online
View Journal | View Issue

Cite this: *Phys. Chem. Chem. Phys.*, 2013, **15**, 15234

Photoinduced charge transport over branched conjugation pathways: donor–acceptor substituted 1,1-diphenylethene and 2,3-diphenylbutadiene

Cornelis A. van Walree,*[ab] Bas C. van der Wiel[c] and René M. Williams[d]

Received 22nd May 2013,
Accepted 10th July 2013

DOI: 10.1039/c3cp52148f

www.rsc.org/pccp

Photoinduced charge transport in 1,1-diphenylethene and 2,3-diphenylbutadiene functionalized with an electron donating dimethylamino group and an electron accepting cyano group is reported. UV-spectroscopy reveals that in these compounds, which incorporate a cross-conjugated spacer, a direct charge transfer transition is possible. It is shown by application of the generalized Mulliken–Hush approach that introduction of an additional branching point in the π-electron spacer (*i.e.*, when going from the 1,1-diphenylethene to the 2,3-diphenylbutadiene) leads to only a moderate reduction (68–92%) of the electronic coupling between the ground and the charge separated state. The σ-electron system is however likely to be dominant in the photoinduced charge separation process.

Introduction

Charge transport is the key process in molecular electronics and a variety of optoelectronic phenomena. In organic compounds and materials the feasibility and the rate of the transport are largely determined by the nature of the path over which it occurs.[1–3] The effectiveness of a given pathway can be assessed by substitution with electron donating and accepting functionalities at the termini and the subsequent evaluation of the electronic interaction between these entities. Thus, the occurrence of photoinduced charge separation and charge recombination processes in electron donor–acceptor compounds is often diagnostic of the ability of the intervening molecular framework to transmit charges while the dynamics of these processes are indicative of the nature of the electron transport mechanism.[4,5]

Photoinduced charge transfer (CT) in a vast amount of donor-bridge-acceptor compounds has been investigated. The various types of electronic interactions that are inherent to the intervening medium between the donor and the acceptor can be described as resulting from *e.g.* linear π-conjugation,[4,6] σ-interactions,[7] homoconjugation,[8] and foldamer coupling in helical bridges.[9] Photoinduced charge transfer in donor–acceptor substituted compounds with a branched (bifurcated) π-spacer has however received little attention.[10–17] Branched π-systems, also referred to as cross-conjugated systems,[18] are intriguing since they represent topological two-dimensional conducting systems and incorporate multiple conjugation paths. As such, they can give rise to quantum interference,[19–25] *i.e.* the interaction between different conjugation paths. This can manifest itself in two ways, *i.e.*, by communication *via* a through-bond or a through-space mechanism.[26] The availability of multiple conjugation paths is thus of great importance for the development of two-dimensional molecular conduction systems and molecular switches, particularly when radical ions or excited states are involved.[27,28] Furthermore, an electron mobility among the highest observed has been reported for an organic field effect transistor based on a cross-conjugated material.[29] Donor and/or acceptor substituted branched π-systems are moreover useful for two-photon absorption purposes.[30,31]

An important and hitherto largely unanswered question is how efficiently charge carriers can be transported over branching points in bifurcated π-systems; the feasibility of charge transport over π-systems containing multiple branching sites has to our knowledge hardly been explored. Here we address these issues with the use of the dimethylamino-cyano functionalized 1,1-diphenylethene **DA1** and 2,3-diphenylbutadiene **DA2** (Chart 1). In these compounds each olefinic carbon atom bonded to a phenylene group forms the branching point of linear π-systems; the bridge in **DA2** is an extension of the one in **DA1**. The charge transport ability of the branched conduction paths is addressed by considering the absorption and fluorescence properties of **DA1** and **DA2**, which allow the evaluation of the electronic coupling and the communication between the donor and acceptor sites. As such, this study is an extension of our earlier work[32,33] on these cross-conjugated systems.

[a] *Flinders Centre for Nanoscale Science and Technology, School of Chemical and Physical Sciences, Flinders University, GPO Box 2100, Adelaide 5001, Australia*
[b] *Department of Chemistry, Utrecht University, Sorbonnelaan 16, 3584 CA, Utrecht, The Netherlands. E-mail: c.a.vanwalree@uu.nl*
[c] *BELECTRIC OPV GmbH, Landgrabenstrasse 94, 90443, Nürnberg, Germany*
[d] *Molecular Photonics Group, Van 't Hoff Institute of Molecular Sciences, University of Amsterdam, Science Park 904, 1090 GD Amsterdam, The Netherlands*

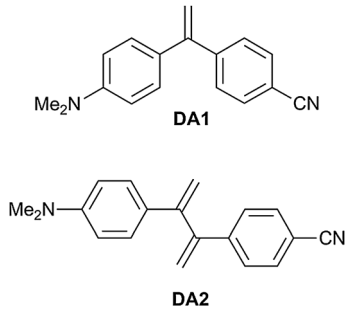

Chart 1 Molecular structures of **DA1** and **DA2**.

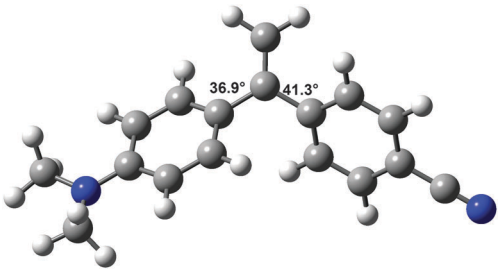

Fig. 1 6-311G** DFT/B3LYP calculated structure of **DA1**. Magnitudes of some torsion angles are indicated.

Results and discussion

Synthesis

The synthesis of **DA1** has been reported previously.[33] Donor–acceptor substituted 2,3-diphenylbutadiene **DA2** was synthesized starting with a benzoin condensation of 4-*N*,*N*-dimethylaminobenzaldehyde and 4-bromobenzaldehyde, giving benzoin **1** (Scheme 1). It is known from the literature that exclusive formation of the benzoin isomer occurs in which the carbonyl group is adjacent to the dimethylaminophenyl fragment.[34] Nevertheless, the other possible isomer also would have given benzil **2** in the next step, oxidation by copper(II)sulfate in pyridine. The oxidation was followed by a twofold Wittig reaction with methylenetriphenylphosphorane to obtain disubstituted 2,3-diphenylbutadiene **3**. Finally, bromide **3** was converted into **DA2** by a palladium-catalyzed reaction with trimethylsilylcyanide.[35]

Molecular structures

Since the molecular geometry can have a strong effect on CT processes,[36] the structures of **DA1** and **DA2** are of interest. Unsubstituted 2,3-diphenylbutadiene was previously found to adopt a somewhat surprising s-*gauche* conformation in the solid state, with a torsion angle of 55.6° around the butadiene single bond.[37,38] MP2 and DFT calculations supported that this compound possesses an s-*gauche* minimum, and also revealed the presence of an s-*trans* minimum, which is somewhat (depending on the calculation method up to 1.47 kcal mol^{-1}) higher in energy.[38,39]

The structures of **DA1** and **DA2** were investigated with 6-311G** DFT/B3LYP calculations. In the optimized structure of **DA1** (E = −481 363.76 kcal mol^{-1}), the torsion angles between the double bond and the aniline and cyanophenyl groups amount to 36.9° and 41.3°, respectively (Fig. 1). These values are close to those found for 1,1-diphenylethene.[27] In common with 2,3-diphenylbutadiene, for **DA2** two minima were found (Fig. 2). The global minimum is represented by a structure with an s-*gauche* geometry around the central single bond (torsion angle 55.8°, E = −529 943.14 kcal mol^{-1}), while a minimum with a central torsion angle of 152.2° (E = −529 942.58 kcal mol^{-1}) occurs as well. The limited energy difference between the two conformations indicates that two conformations might be present under ambient conditions, the s-*gauche* structure being dominant. The s-*gauche* minimum is further characterized by torsion angles of

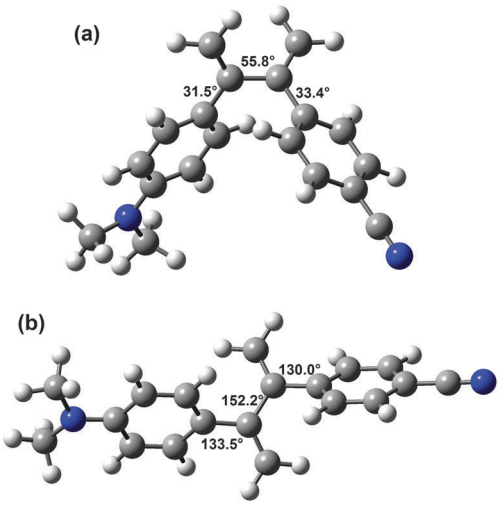

Fig. 2 6-311G** DFT/B3LYP calculated structures of **DA2** in the s-*gauche* (a) and s-*trans* (b) minima. Magnitudes of some torsion angles are indicated.

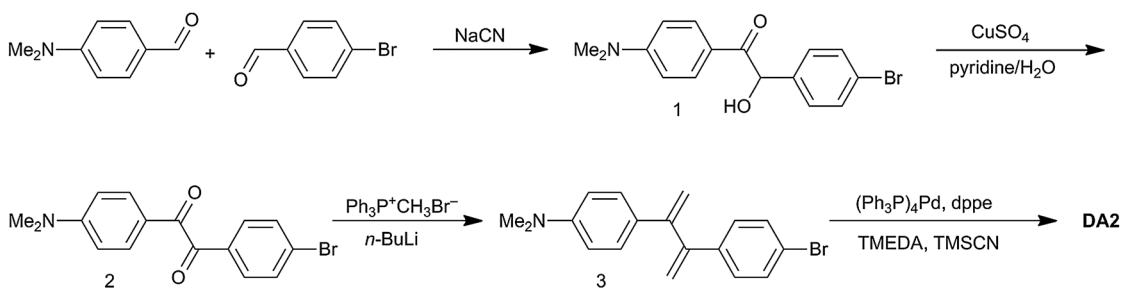

Scheme 1 Synthesis of **DA2**.

31.5° between the aniline moiety and the adjacent double bond, and 33.4° between the cyanophenyl part and the adjacent double bond. The other structure contains torsion angles of 133.5° and 130.0° between the double bonds and the aniline and the cyanophenyl moiety, respectively. The calculated conformations are in agreement with geometries calculated by Limacher and Lüthi.[39]

The lowest energy structure of **DA2** is thus different from the s-*trans* structure that was initially assumed,[32] and this might have a bearing on the understanding of the behaviour of the compound. In the butterfly-like s-*gauche* geometry **DA2** possesses a compact structure, whereas in the s-*trans* conformation the geometry is extended. In fact, in the former geometry the donor and acceptor parts are closer together than in **DA1**. The N–N distance is 10.9 Å in **DA1** and 9.4 Å in s-*gauche* **DA2** (while it is 13.2 Å in s-*trans* **DA2**). This is also exemplified by the 6-311G** DFT/B3LYP ground state dipole moments, which are 5.41 and 7.33 D for s-*gauche* **DA2** and **DA1**, respectively. The dipole moment of s-*trans* **DA2** is 7.98 D.

Absorption and fluorescence spectroscopy

UV spectra of **DA1** and **DA2** are depicted in Fig. 3, together with spectra of the reference compounds 4-*N*,*N*-dimethylaminostyrene and 4-cyanostyrene. The spectra of the donor–acceptor compounds exhibit local cyanophenyl ^1L_a type transitions at 258–265 nm and *N*,*N*-dimethylaniline ^1L_a type transitions at 280–298 nm.[33] For both **DA1** and **DA2** a charge transfer (CT) absorption band is present; it appears as a shoulder at the red edge of the dimethylaniline ^1L_a transition. In the difference spectra (Fig. 3b) the CT absorptions are found at 341 and 340 nm for **DA1** and **DA2**, respectively. For **DA1** a second CT absorption seems to be present near 310 nm, but the actual maximum may be obscured by the negative absorption at 290 nm. This signal possibly reflects a CT absorption in another conformation.

As the stabilization of the CT state by Coulomb attraction between the separate charges depends on the donor–acceptor distance, the minor difference between the CT absorption maxima (341 *vs.* 340 nm) is not unexpected when the donor–acceptor distance is similar, as is the case for **DA1** and s-*gauche* **DA2**. Note however that the behaviour of a CT absorption as a function of chain length also depends on the combination of donor–acceptor strength and the conjugation path,[6] and it could be that compounds **DA1** and **DA2** are in a regime where the energy of the (Franck–Condon) CT state is only weakly dependent on the chain length. This might be in line with the sometimes complex electronic spectra of cross-conjugated systems, which do not always reflect the extent of conjugation.[40–42] If the CT absorption of **DA2** at 340 nm arises in the s-*gauche* conformation, then the band near 310 nm could represent the CT absorption in the s-*trans* conformation.

The presence of CT absorption bands implies that a significant ground state interaction between the donor and acceptor chromophores is present. For **DA1** and other compounds with a bridge consisting of a single sp^2 hybridized carbon atom this was derived earlier,[10,12–14,33] but as far as we are aware **DA2** is the first compound for which an interaction over two branching points

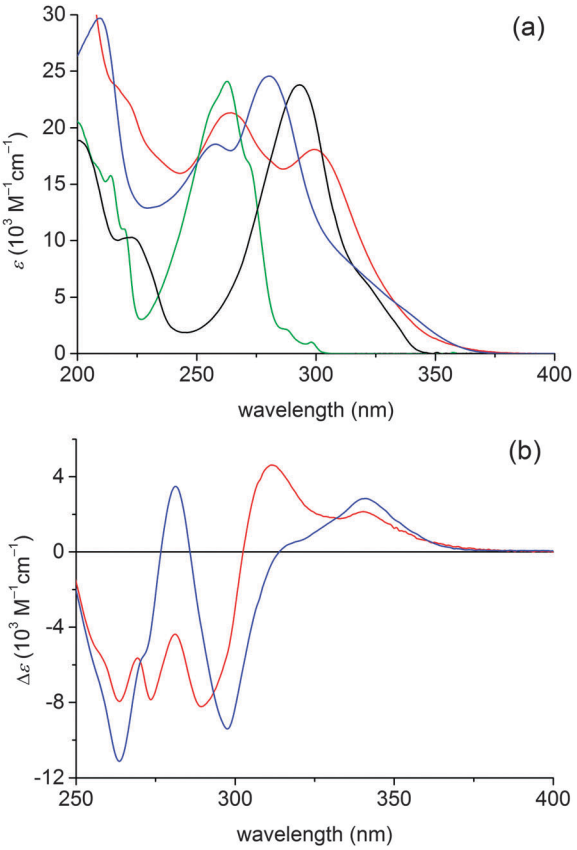

Fig. 3 (a) UV spectra of **DA1** (blue) and **DA2** (red) along with spectra of the reference chromophores 4-*N*,*N*-dimethylaminostyrene (black) and 4-cyanostyrene (green) in cyclohexane. (b) UV difference spectra obtained by subtraction of the spectra of the reference chromophores 4-*N*,*N*-dimethylaminostyrene and 4-cyanostyrene from the spectra of **DA1** (blue) and **DA2** (red).

has been reported.[32] As judged from the absorption coefficient of the CT band in the difference spectrum, $\varepsilon = 2140\ M^{-1}\ cm^{-1}$ and $\varepsilon = 2800\ M^{-1}\ cm^{-1}$ for **DA1** and **DA2**, respectively, the coupling is moderate. The negative peaks in the wavelength range 290–300 nm and near 263 nm in Fig. 3b suggest that the CT transitions borrow their intensity from the local *N*,*N*-dimethylaniline and cyanophenyl ^1L_a transitions.[43]

Fluorescence spectra of **DA1** and **DA2** in various solvents are shown in Fig. 4 (tabulated data were reported previously).[32] The fluorescence is strongly solvatochromic, revealing that in both compounds a highly dipolar CT excited state is generated upon excitation. The fluorescence maxima can be plotted against the solvent polarity according to the well-known Lippert–Mataga relationship (Fig. 5). Since **DA1** and **DA2** have substantial ground state dipole moments, the following form is most appropriate:[44,45]

$$\nu_{abs} - \nu_{fl} = C + \frac{2\Delta\mu^2}{hc\rho^3} \times \Delta f \qquad (1a)$$

$$\text{with } \Delta f = \frac{\varepsilon_s - 1}{2\varepsilon_s + 1} - \frac{n^2 - 1}{2n^2 + 1} \qquad (1b)$$

in which ν_{abs} and ν_{fl} represent the absorption and the fluorescence wavenumber, respectively, $\Delta\mu$ the difference in (static) dipole

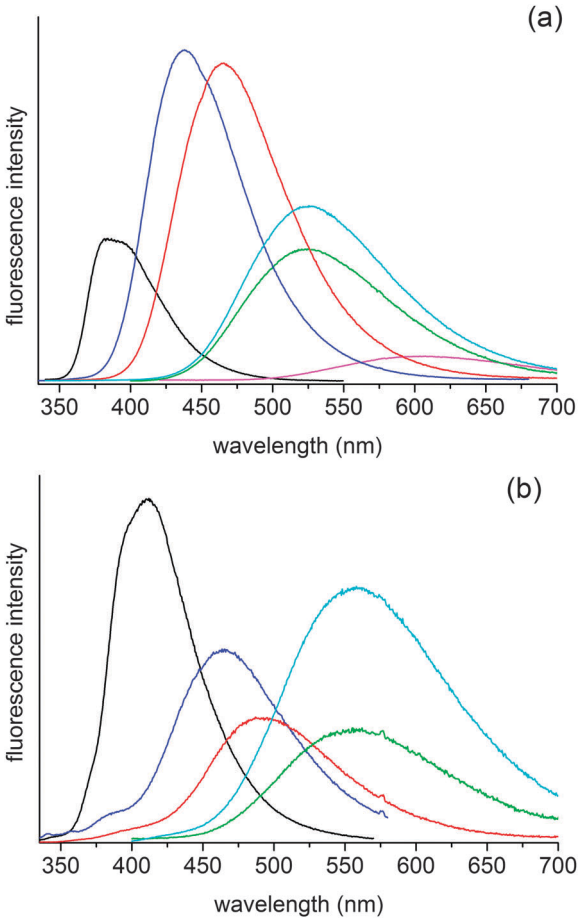

Fig. 4 Fluorescence spectra of **DA1** (a) and **DA2** (b) in various solvents. Maxima of **DA1** are situated at 389.0 (cyclohexane, black), 437.5 (di-*n*-butyl ether, blue), 465.5 (diethyl ether, red), 525.5 (ethyl acetate, green), 525.5 (THF, cyan) and 605.0 nm (acetonitrile, magenta). Maxima of **DA2** are found at 410.5 (cyclohexane, black), 464.0 (di-*n*-butyl ether, blue), 493.0 (diethyl ether, red), 556.0 (ethyl acetate, green) and 558.0 nm (THF, cyan). In acetonitrile **DA2** is non-fluorescent.

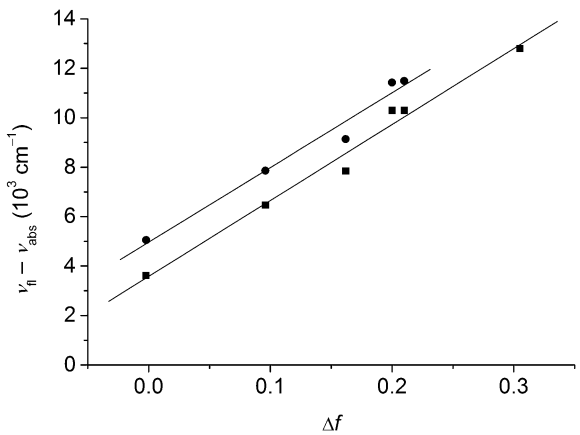

Fig. 5 Solvatochromism of **DA1** (squares) and **DA2** (spheres).

moment of the CT and the ground state, h the Planck constant, c the light velocity and ρ the solute cavity radius. The solvent polarity parameter Δf is a function of the dielectric constant ε_s and the refractive index n (eqn (1b)).[46] The ν_{abs} value obtained in cyclohexane was used for all other solvents. For **DA1** a slope $2\Delta\mu^2/hcp^3$ of 30.7 ± 2.0 × 10^3 cm^{-1}, an intercept C of 3.58 ± 0.38 × 10^3 cm^{-1} and a correlation coefficient R of 0.991 were obtained. For **DA2** fit results were $2\Delta\mu^2/hcp^3$ = 30.2 ± 2.8 × 10^3 cm^{-1}, C = 4.96 ± 0.44 × 10^3 cm^{-1} and R = 0.986. The solvatochromic fits have very similar slopes, and the major difference between **DA1** and **DA2** is not situated in the slope $2\Delta\mu^2/hcp^3$ but in an offset of the fluorescence of the latter by some 1200 cm^{-1} (1200 cm^{-1} reflects the average difference between the fluorescence wavenumbers; a difference based on the intercepts gives a somewhat deviating value because of the extrapolation, and also contains a contribution of the small difference in ν_{abs} between **DA1** and **DA2**).

The equal slopes suggest that the emitting species of **DA1** and **DA2** are homologous; the structure in the excited state must be very similar. **DA1** is a fairly rigid molecule in which only rotation along the two phenylene–vinylidene single bonds is possible. **DA2** has more conformational freedom, which is of interest since Coulombic attraction between the radical ion sites might induce conformational changes, particularly in nonpolar solvents.[47–50] Because of the very similar solvatochromic sensitivities of **DA1** and **DA2** and the fact that the solvatochromism of **DA2** is convincingly described by a single straight line, we tend to think that such conformational changes do not occur. In the excited state **DA2** must adopt a structure similar to the s-*gauche* structure and which bears a strong resemblance to that of **DA1**. Fast processes (down to the order of 30 ps) reflecting potential conformational changes were not observed in time-resolved fluorescence measurements. If the difference UV-signal near 310 nm corresponds to the CT absorption in the s-*trans* conformation, the change into the compact conformation must be very fast. Note that in the fluorescence spectra of **DA2** in di-*n*-butyl and di-*n*-pentyl ether a weak band near 380 nm is visible. In common with the behaviour of 1-(4-*N*,*N*-dimethylaminophenyl)-1-phenylethene,[33] this signal is assigned to local aniline type fluorescence. Using cavity radii of 4.5 and 4.7 Å (ref. 51) from the solvatochromic fits $\Delta\mu$ values of 16.7 and 17.6 D are calculated for **DA1** and **DA2**, respectively.

As described above, the fluorescence maxima of **DA2** are systematically situated below those of **DA1** by some 1200 cm^{-1}, meaning that the CT state of **DA2** is more stable than that of **DA1**. In order to rationalize this difference, it is instructive to consider which terms determine the energy of a CT state. According to the expression[52,53]

$$h\nu_{fl} = \Delta G^0_{RIP} - \lambda_i - \lambda_s \quad (2a)$$

with

$$\Delta G^0_{RIP} = eE_{ox}(D) - eE_{red}(A) - \frac{e^2}{4\pi\varepsilon_0\varepsilon_s R_{DA}} + \frac{e^2}{8\pi\varepsilon_0}\left(\frac{1}{r_D} + \frac{1}{r_A}\right)\left(\frac{1}{\varepsilon_s} - \frac{1}{36.9}\right) \quad (2b)$$

the CT fluorescence energy is related to the nuclear and solvent reorganization energies λ_i and λ_s, respectively, the donor oxidation potential $E_{ox}(D)$ and the acceptor reduction potential $E_{red}(A)$.

The last terms in eqn (2b) account for electrostatic and solvation effects and depend on the solvent dielectric constant, donor and acceptor radical cat- and anion radii r_D and r_A, and the donor–acceptor distance R_{DA}. Differences between **DA1** and **DA2** in the last term are assumed to be negligible since all data are virtually identical for the two compounds. The term containing R_{DA} may be of some importance though. In the 6-311G** DFT/B3LYP ground state geometries, the N–N distance is 10.9 Å for **DA1** and 9.4 Å for s-*gauche* **DA2**. In cyclohexane (ε_s = 2.02)[46] the term would favour s-*gauche* **DA2** relative to **DA1** by 840 cm^{-1}, while in THF the difference would be 230 cm^{-1}. It is difficult to exactly assess the contribution of the R_{DA} term to the CT energy offset since excited sate geometries will be somewhat different from ground state geometries. The observation that the solvatochromic fits run almost parallel suggests that not too much credit should be paid to this term (and might also be interpreted to imply that R_{DA} distances must be similar).

The first oxidation potentials of **DA1** and **DA2** were both determined to be 0.65 V *vs.* SCE by cyclic voltammetry in acetonitrile, while the respective first reduction potentials are −2.16 and −2.13 V *vs.* SCE, respectively.[54] The small differences between the redox potentials of **DA1** and **DA2** thus account for another portion, albeit small, of the offset of 1200 cm^{-1} (0.03 eV corresponds to 242 cm^{-1}) in the CT state energies. Therefore, the largest contribution to the onset must arise from a difference in reorganization energy. The solvent reorganization energy is determined by[53]

$$\lambda_s = \frac{{\mu_{CT}}^2}{4\pi\varepsilon_0\rho^3}\left(\frac{\varepsilon_s - 1}{2\varepsilon_s + 1} - \frac{n^2 - 1}{2n^2 + 2}\right) \quad (3)$$

and cannot differ substantially in a given solvent since the slopes of the solvatochromic fits were found to be very similar. This implies that the nuclear reorganization energy is mainly responsible for the difference between CT state energies. This is consistent with the expectation that the largest reorganization energy should be found for the compound that has more modes available for structural changes, *i.e.* **DA2**. The fluorescence band widths partly support this idea. In the solvents cyclohexane, di-*n*-butyl ether and diethyl ether they amount to 3880, 4220 and 4230 cm^{-1} for **DA2**, respectively, while those of **DA1** are 3660, 3930 and 4020 cm^{-1}. This is in line with the expectation that they are broader for the compound with the larger reorganization energy.[52,53,55] However, in THF and ethyl acetate the fluorescence bands of **DA1** are broader (4230 and 4380 cm^{-1} *vs.* 4140 and 4250 cm^{-1} in THF and ethyl acetate, respectively).

Electronic couplings

In a two-level model, the coupling H_{DA} between the ground state and the CT excited state can be obtained from the generalized Mulliken–Hush expression[56]

$$H_{DA} = \frac{\mu_{ge}\nu_{abs}}{\left(\Delta\mu^2 + 4{\mu_{ge}}^2\right)^{1/2}} \quad (4)$$

in which μ_{ge} is the transition dipole moment, $\Delta\mu$ is the difference in (static) dipole moment between the CT and the ground state and ν_{abs} is the vertical CT absorption wavenumber. For **DA1** and **DA2** the $\Delta\mu$ values are already available from the fluorescence solvatochromism. The transition dipole moment μ_{ge} is obtained from

$$\left|\mu_{ge}\right|^2 = \frac{3he^2}{8\pi^2 cm_e}\frac{f}{\nu_{abs}} \quad (5)$$

with $3he^2/8\pi^2 cm_e = 2.367 \times 10^{-51}$ C^2 m and ν_{abs} is given in m^{-1}. There are two ways to obtain the oscillator strength *f*. First, it is given by the integrated CT absorption band:

$$f = 4.32 \times 10^{-9}\ \varepsilon_{max}\Delta\nu_{1/2} \quad (6)$$

where the bandwidths $\Delta\nu_{1/2}$ are preferably taken at the red side of the CT band. Alternatively, electronic couplings can be obtained from fluorescence data.[55,57] The fluorescence quantum yield and lifetime define the radiative rate constants by $k_{rad} = \Phi_{fl}/\tau$, which is related to the oscillator strength by

$$f = \frac{1.5k_{rad}}{n^3{\nu_{av}}^2} \quad (7)$$

Here ν_{av} denotes the mean emission wavenumber over the fluorescence spectrum, which can be extracted from the reduced spectrum.[55] After evaluation of *f*, the transition dipole moment and the electronic coupling are obtained from eqn (5) and (4), respectively, albeit that now ν_{av} instead of ν_{abs} is applied.

The CT bands of **DA1** and **DA2** have absorption coefficients ε_{max} of 2800 and 2140 M^{-1} cm^{-1}, respectively, while the bandwidths are 2000 and 1840 cm^{-1} (Fig. 3b). Application of eqn (6), (5) and (4) then leads to couplings H_{DA} given in Table 1. Fluorescence data and couplings derived from them are also compiled in this table. In cyclohexane, the couplings obtained from the absorption and fluorescence data are rather similar. This seems to be partly fortuitous, since the differences in

Table 1 Fluorescence data and couplings between the ground state and the CT states in **DA1** and **DA2**

	DA1					**DA2**				
	$\nu_{av}/10^3$ cm^{-1}	Φ_{fl}	τ_{fl}/ns	$f/10^{-2}$	H_{DA}/cm^{-1}	$\nu_{av}/10^3$ cm^{-1}	Φ_{fl}	τ_{fl}/ns	$f/10^{-2}$	H_{DA}/cm^{-1}
Cyclohexane[a]				2.4	2290				1.7	1840
Cyclohexane[b]	24.76	0.087	2.2	3.33	2460	23.56	0.084	4.4	1.78	1680
Diethyl ether[b]	20.58	0.19	18.5	1.46	1502	19.69	0.044	6.7	1.03	1170
THF[b]	18.16	0.13	16.9	1.24	1300	17.30	0.062	9.0	1.22	1190

[a] From absorption spectrum (eqn (6), (5) and (4)); ε was taken from Fig. 3b, absorption band widths are 2000 (**DA1**) and 1840 (**DA2**) cm^{-1}. [b] From radiative decay rates (eqn (7), (5) and (4)).

oscillator strength are compensated by the difference in absorption and fluorescence energy. Nevertheless, the data are in reasonable agreement. The fluorescence data show that with increasing solvent polarity the couplings decrease. This does not take away that in the most polar solvent considered, THF, the magnitude of the couplings is still substantial, even when two branching points are present. In each solvent the coupling in **DA1** is larger than in **DA2**, but the decrease of H_{DA} when going from one to two branching points is surprisingly modest. The ratio of the couplings varies between 68% in cyclohexane and 92% in THF.

The most significant data are presumably those obtained in THF. The couplings in cyclohexane and diethyl ether should be treated with some caution since intensity borrowing from local transitions by the CT transitions occurs in the compounds under investigation.[33,43] In particular the radiative decay of the CT states in cyclohexane will be strongly affected by the properties of the locally excited aniline type ^1L_a state, as in this nonpolar solvent these states are close in energy. Hence, couplings in the nonpolar solvents are expected to be too large, and a three state model would be more appropriate.[43,58–60] However, in a computational study on multistate effects in the generalized Mulliken–Hush treatment the two state model was shown to be applicable to dimethylaminobenzonitrile, which was considered to be an extreme test case.[60] Significant state mixing was shown to have a marginal effect on interstate couplings. Moreover, state energies and the nature of the CT state are similar for **DA1** and **DA2**, so that the amount of intensity borrowing is not too different for the two compounds. The relative differences between **DA1** and **DA2** are therefore considered to be meaningful.

General discussion and conclusions

There is a significant electronic interaction between donor and acceptor functionalities in the branched π-systems considered here. While it has been established that the cross-conjugation pattern in diphenylethene strongly decreases the donor–acceptor coupling,[16] the remaining interaction certainly is substantial and implies that charge transport is well possible in bifurcated π-systems. Moreover, in these types of compounds additional branching points can be inserted at the cost of only a limited extent of donor–acceptor interaction. This suggests molecular wire behaviour, *i.e.* weak attenuation of the electronic coupling with the distance.[4] It is of interest to note that molecular wire behaviour is often observed for systems based on other modes of conjugation than linear π-conjugation.[61,62] In this wire-like behaviour, quantum interference can play a significant role,[26] but its precise nature in compounds like **DA1** and **DA2** is difficult to assess. It involves answering the question as to which mechanism underlies the charge transport in the compounds under investigation. Given the structures of the compounds, both through-space and through-bond interactions may be operative. The importance of through-bond interactions is indicated by the observation that H_{DA} is larger for **DA1** than for **DA2**. If only a through-space mechanism would be active, a larger value would have been expected for **DA2**, which has a shorter donor–acceptor separation.

In the through-bond mechanism, effects in both the π- and σ-electron systems may contribute. From a NBO population analysis Limacher and Lüthi revealed a ground state effect on the π-electrons of compound **DA2**.[39] Butler-Ricks *et al.* showed that in a donor–acceptor substituted diphenylethene the σ-electron system may be dominant in charge transport.[16] In this respect it is of interest to compare the behavior of **DA1** with that of data for molecules containing an *N*,*N*-dimethylaniline donor and a cyanophenyl acceptor separated by a bridge consisting of a single sp^3 carbon atom like compound **1C**.[43,63] The ε-value of the charge transfer absorption in **1C** is 2500 M^{-1} cm^{-1}, which is close to that for **DA1**. Evaluation of the coupling between the ground and CT states for **1C** with the generalized Mulliken–Hush method gives H_{DA} = 2190 cm^{-1} in diethyl ether (ν_{av} = 23 700 cm^{-1}, f = 0.031 and $\Delta\mu$ = 17.7 D) and H_{DA} = 1420 cm^{-1} in ethyl acetate (ν_{av} = 20 900 cm^{-1}, f = 0.014 and $\Delta\mu$ = 17.7 D). The higher H_{DA} values for **1C** in comparison to **DA1** might be explained by the somewhat shorter donor–acceptor distance in **1C** (N–N distance 10.3 Å *vs.* 10.9 Å) and an increased through-space contribution. More importantly, the small difference between the couplings in **DA1** and **1C** indicates that the effect of the double bond is minor and that the σ-electron system is dominant in photoinduced charge transfer processes in the cross-conjugated compounds indeed.

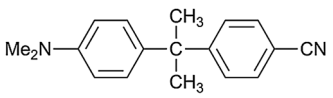

1C

In conclusion, it has been shown that charge can be transported efficiently over cross-conjugated pathways incorporating one or two branching points. This reveals that 1,1-diphenylethene and 2,3-diphenylbutadiene systems can participate in 2-dimensional conducting systems, in which charge carriers can be conducted along linear- and cross-conjugated pathways. Herewith it should be realized that **DA1** and **DA2** are not planar, and that it is difficult to separate through-bond and through-space effects. Moreover, the σ-system is likely to be dominant.

Experimental section

General

Reactions involving organolithium reagents were conducted under nitrogen using standard Schlenk techniques. Starting materials and reagents were obtained from commercial sources and used as received. Solvents generally were distilled before use; dry diethyl ether and toluene were obtained by distillation from sodium-benzophenone. Column chromatography was performed with Acros silica (0.035–0.070 mm, pore diameter *ca.* 6 nm). For gas chromatography use was made of a Varian 3400 gas chromatograph equipped with an Alltech EC-5 capillary column. NMR spectra were recorded in $CDCl_3$ using a Bruker AC-300 spectrometer (operating at 300 MHz for ^{1}H NMR and 75 MHz for ^{13}C NMR) and are calibrated to TMS as internal standard. IR spectra were taken in ATR mode on neat samples on a Perkin-Elmer Spectrum One FT-IR spectrometer equipped

with a Universal ATR Sampling accessory. Melting points were determined on a Mettler FP5/FP51 photoelectric apparatus. Elemental analysis was carried out at Kolbe Microanalytisches Laboratorium, Mülheim an der Ruhr, Germany.

UV spectra were collected on Cary 1 or Cary 5 spectrophotometers in spectrophotometric grade solvents. Fluorescence spectra were obtained on a Spex Fluorolog instrument.[33] Fluorescence quantum yields[64] were determined relative to anthracene (Φ_{fl} = 0.27) upon 310 nm excitation. Fluorescence lifetimes were determined using a streak camera system described elsewhere.[65] Cyclic voltammetry was conducted using an EG&G PAR model 63A potentiostat/galvanostat in acetonitrile with tetrabutylammonium hexafluorophosphate as a supporting electrolyte. Potentials were calibrated against SCE by recording a voltammogram of internal ferrocene ($E_{1/2}$ = +0.31 V *vs.* SCE).

DFT B3LYP/6-311G** calculations were performed with the Gaussian09 package.[66] Stationary points were characterized as minima by Hessian calculations.

The synthesis of **DA1** has been reported elsewhere.[33]

4-Bromo-4′-*N*,*N*-dimethylaminobenzoin (1). In a nitrogen atmosphere, a solution of 4-bromobenzaldehyde (17.45 g, 94.3 mmol), 4-*N*,*N*-dimethylaminobenzaldehyde (13.39 g, 89.8 mmol) and NaCN (1.92 g, 39.2 mmol) in 180 mL ethanol was refluxed for 21 hours. The reaction mixture was concentrated under reduced pressure, after which water was added. The aqueous phase was extracted with dichloromethane (3 × 75 mL). Drying with calcium chloride, filtration and evaporation of the combined organic layers afforded 29.73 g crude product, composed of (amongst others) at least 22% **1**, 42% 4-dimethylaminobenzaldehyde and 2% 4-bromobenzaldehyde as determined by gas chromatography. This was used without further purification.

A pure sample of **1** was obtained as a white crystalline solid by repeated crystallization from ethanol and methanol. mp 115 °C. NMR: $\delta_H(CDCl_3)$ 7.80 (2H, d, ^3J 9.09, Ar-H), 7.43 (2H, d, ^3J 8.52, Ar-H), 7.22 (2H, d, ^3J 8.52, Ar-H,), 6.57 (2H, d, ^3J 9.09, Ar-H), 5.80 (1H, d, ^3J 6.06, C*H*(OH)), 4.78 (1H, d, ^3J 6.06, OH), 3.03 (6H, s, NMe_2); $\delta_C(CDCl_3)$ 195.6 (q, C═O), 154.1 (q, *C*-NMe_2), 139.8 (q), 132.2, 131.7, 129.5, 122.4 (q), 120.6 (q), 110.8, 74.6 (COH), 40.1 (NMe_2). IR: ν_{max}/cm^{-1} 3389, 2913, 1821, 1648, 1593, 1549, 1485, 1375, 1255, 1196, 1169, 1084, 1013, 976, 949, 808, 755.

4-Bromo-4′-*N*,*N*-dimethylaminobenzil (2). A suspension of crude **1** (29.73 g, containing at least 19.7 mmol **1**) and copper(II) sulfate pentahydrate (92.00 g, 368.5 mmol) in a mixture of pyridine and water (4 : 1 v/v, 250 mL) was refluxed for 21 hours. Water (250 mL) was added to dissolve the copper salts and the resulting slurry was extracted with ether (3 × 350 mL). The combined organic layers were dried on magnesium sulfate, filtered and evaporated under reduced pressure. The crude product (29.85 g) was purified by Kugelrohr distillation at 0.05 mbar, discarding the fractions boiling below 120 °C. Hot ethanol was added to the residue and insoluble impurities were removed by filtration. Recrystallization from ethyl acetate gave 7.13 g (21.5 mmol) of a brown-yellow solid. Purity 96% by GC.

Following the same procedure, pure **2** was obtained in 83% yield from the small amount of pure **1**. mp 145 °C. NMR: $\delta_H(CDCl_3)$ 7.87–7.81 (2 × 2H, 2 × d, Ar-H), 7.62 (2H, d, ^3J 8.52, Ar-H), 6.67 (2H, d, ^3J 9.36, Ar-H), 3.10 (6H, s, NMe_2); $\delta_C(CDCl_3)$ 194.5 (q, C═O), 191.8 (q, C═O), 154.7 (q, *C*-NMe_2), 132.7 (q), 132.4, 132.3, 131.4, 129.9 (q), 120.7 (q), 111.2, 40.2 (NMe_2). IR: ν_{max}/cm^{-1}: 2915, 1671, 1637, 1580, 1480, 1374, 1230, 1167, 1067, 873, 830, 810, 743.

2-(4-Bromophenyl)-3-(4-*N*,*N*-dimethylaminophenyl)-1,3-butadiene (3). *n*-Butyllithium in hexanes (22.5 mL of a 1.6 M solution, 36 mmol) was added to a suspension of methyltriphenylphosphonium bromide (11.83 g, 33.1 mmol) in THF (80 mL) at 0 °C. After one hour, a solution of **2** (5.00 g, 15.05 mmol) in THF (50 mL) was added dropwise. The reaction mixture was refluxed for 21 hours, quenched with water (100 mL), and extracted with ether (3 × 100 mL). The combined ether layers were washed with water (2 × 100 mL), dried with magnesium sulfate, filtered and concentrated under reduced pressure. The mixture was subjected to flash chromatography (silica, CH_2Cl_2). Subsequently, a side product was removed by crystallization from toluene (*ca.* 3 g in 15 mL). The mother liquor was dried under reduced pressure and part of it was subjected to column chromatography (silica, 7 : 1 v/v hexane : ether) to give 0.80 g of a yellow solid containing 66% **3** and 13% triphenylphosphine as the main components (GC). This mixture was used without further purification. NMR: $\delta_H(CDCl_3)$ 7.36 (2H, d, ^3J 8.52, Ar-H), 7.28 (2H, d, ^3J 8.52, Ar-H), 7.26 (2H, d, ^3J 8.79, Ar-H), 6.60 (2H, d, ^3J 8.79, Ar-H), 5.53 (1H, d, ^2J 1.65, C═CH), 5.45 (1H, d, ^2J 1.65, C═CH), 5.35 (1H, d, ^2J 1.65, C═CH), 5.13 (1H, d, ^2J 1.65, C═CH), 2.91 (6H, s, NMe_2). GC-MS (EI): *m*/*z* 329 + 327 (M^+), 285, 283, 248, 207–204, 172, 134 (100%), 124, 101, 77.

2-(4-Cyanophenyl)-3-(4-*N*,*N*-dimethylaminophenyl)-1,3-butadiene (DA2). A flask charged with tetrakis(triphenylphosphine)-palladium(0) (46.16 mg, 39.9 μmol) and 1,5-bis(diphenylphosphino)pentane (17.92 mg, 40.7 μmol) was purged with nitrogen. A mixture of **3** (0.5 g, containing 1.0 mmol **3**), toluene (2 mL) and TMEDA (60 μL) was added. A 1 M solution of trimethylsilylcyanide in toluene (4 mL) was added dropwise *via* a syringe pump at a rate of 0.2 mmol h^{-1} at reflux temperature.[35] After 20 hours the mixture was cooled, diluted with ether and passed over Celite. This reaction was carried out in the same way with another batch of impure **3** (0.3 g, containing 0.6 mmol **3**). The combined crude products were subjected to column chromatography (silica, 5 : 1 v/v CH_2Cl_2 : $CHCl_3$). This was followed by recrystallization from ethanol to yield 0.17 g (0.62 mmol, 39%) of a yellow solid. mp 132 °C. NMR: $\delta_H(CDCl_3)$ 7.55–7.45 (2 × 2H, 2 × d, Ar-H), 7.21 (2H, d, ^3J 9.06, Ar-H), 6.59 (2H, d, ^3J 9.06, Ar-H), 5.64 (1H, d, ^2J 1.65, C═CH), 5.49 (2 × 1H, 2 × d, C═CH), 5.15 (1H, d, ^2J 1.65, C═CH), 2.92 (6H, s, NMe_2); $\delta_C(CDCl_3)$ 150.3 (q, *C*-NMe_2), 149.1 (q, *C*═CH_2), 148.5 (q, *C*═CH_2), 145.1 (q), 132.2, 128.2, 128.0, 127.1 (q), 119.1 (q, CN), 118.2 (C═*C*H_2), 113.5 (C═*C*H_2), 112.1, 111.0 (q), 40.5 (NMe_2). IR: ν_{max}/cm^{-1} 2888, 2812, 2231, 1610, 1524, 1505, 1362, 1199, 925, 888, 843, 814. Anal. found: C, 83.0; H, 6.6; N, 10.1. Calc. for $C_{19}H_{18}N_2$: C, 83.2; H, 6.6; N, 10.2%.

References and notes

1 M. R. Wasielewksi, *Chem. Rev.*, 1992, **92**, 435–461.
2 O. Wenger, *Acc. Chem. Res.*, 2011, **44**, 25–35.
3 P. F. Barbara, T. J. Meyer and M. A. Ratner, *J. Phys. Chem.*, 1996, **100**, 13148–13168.
4 W. B. Davis, W. A. Svec, M. A. Ratner and M. R. Wasielewski, *Nature*, 1998, **396**, 60–63.
5 G. Pourtois, D. Beljonne, J. Cornil, M. A. Ratner and J.-L. Brédas, *J. Am. Chem. Soc.*, 2002, **124**, 4436–4447.
6 H. Meier, *Angew. Chem., Int. Ed.*, 2005, **44**, 2482–2506.
7 H. Oevering, M. N. Paddon-Row, M. Heppener, A. E. Oliver, E. Cotsaris, J. W. Verhoeven and N. S. Hush, *J. Am. Chem. Soc.*, 1987, **109**, 3258–3269.
8 N. Herrero-García, M. Del Rosario Colorado Heras, M. Del Rosario Torres, I. Fernández and J. Osío Barcina, *Eur. J. Org. Chem.*, 2012, 2643–2655.
9 M. Wolffs, N. Delsuc, D. Veldman, N. Vân Anh, R. M. Williams, S. C. J. Meskers, R. A. J. Janssen, I. Huc and A. P. H. J. Schenning, *J. Am. Chem. Soc.*, 2009, **131**, 4819–4829.
10 C. Bosshard, R. Spreiter, P. Günter, R. R. Tykwinski, M. Schreiber and F. Diederich, *Adv. Mater.*, 1996, **8**, 231–234.
11 C. Eckert, F. Heisel, J. A. Miehé, R. Lapouyade and L. Ducasse, *Chem. Phys. Lett.*, 1988, **153**, 357–364.
12 C. Maertens, C. Detrembleur, P. Dubois, R. Jérôme, C. Boutton, A. Persoons, T. Kogej and J. L. Brédas, *Chem.–Eur. J.*, 1999, **5**, 369–380.
13 R. R. Tykwinski, M. Schreiber, V. Gramlich, P. Seiler and F. Diederich, *Adv. Mater.*, 1996, **8**, 226–231.
14 R. R. Tykwinski, M. Schreiber, R. P. Carlón, F. Diederich and V. Gramlich, *Helv. Chim. Acta*, 1996, **79**, 2249–2281.
15 J. N. Wilson, K. I. Hardcastle, M. Josowicz and U. H. F. Bunz, *Tetrahedron*, 2004, **60**, 7157–7167.
16 A. Butler Ricks, G. C. Solomon, M. T. Colvin, A. M. Scott, K. Chen, M. A. Ratner and M. R. Wasielewski, *J. Am. Chem. Soc.*, 2010, **132**, 15427–15434.
17 N. N. P. Moonen, W. C. Pomerantz, R. Gist, C. Boudon, J.-P. Gisselbrecht, T. Kawai, A. Kishioka, M. Gross, M. Irie and F. Diederich, *Chem.–Eur. J.*, 2005, **11**, 3325–3341.
18 M. Gholami and R. R. Tykwinski, *Chem. Rev.*, 2006, **106**, 4997–5027.
19 C. Patoux, C. Coudret, J.-P. Launay, C. Joachim and A. Gourdon, *Inorg. Chem.*, 1997, **36**, 5037–5049.
20 R. Baer and D. Neuhauser, *J. Am. Chem. Soc.*, 2002, **124**, 4200–4201.
21 A. Cheong, A. E. Roitberg, V. Mujica and M. A. Ratner, *J. Photochem. Photobiol., A*, 1994, **82**, 81–86.
22 G. C. Solomon, D. Q. Andrews, R. P. Van Duyne and M. A. Ratner, *J. Am. Chem. Soc.*, 2008, **130**, 7788–7789.
23 G. C. Solomon, D. Q. Andrews, R. H. Goldsmith, T. Hansen, M. R. Wasielewski, R. P. Van Duyne and M. A. Ratner, *J. Am. Chem. Soc.*, 2008, **130**, 17301–17308.
24 D. Fracasso, H. Valkenier, J. C. Hummelen, G. C. Solomon and R. C. Chieci, *J. Am. Chem. Soc.*, 2011, **133**, 9556–9563.
25 C. M. Guédon, H. Valkenier, T. Markussen, K. Thygesen, J. C. Hummelen and S. J. van der Molen, *Nat. Nanotechnol.*, 2012, **7**, 305–309.
26 M. J. Shephard, M. N. Paddon-Row and K. D. Jordan, *J. Am. Chem. Soc.*, 1994, **116**, 5328–5333.
27 S. Smolarek, A. Vdovin, A. Rijs, C. A. van Walree, M. A. Zgierski and W. J. Buma, *J. Phys. Chem. A*, 2011, **115**, 9399–9410.
28 P. A. Limacher and H. P. Lüthi, *Wiley Interdiscip. Rev.: Comput. Mol. Sci.*, 2011, **1**, 477–486.
29 R. P. Ortiz, A. Facchetti, T. J. Marks, J. Casado, M. Z. Zgierski, M. Kozaki, V. Hernández and J. T. L. Navarrete, *Adv. Funct. Mater.*, 2009, **19**, 386–394.
30 E. Zojer, D. Beljonne, P. Pacher and J.-L. Bredas, *Chem.–Eur. J.*, 2004, **10**, 2668–2680.
31 T.-C. Lin, S.-J. Chung, K.-S. Kim, X. Wang, G. S. He, J. Swiatkiewicz, H. E. Pudavar and P. N. Prasad, *Adv. Polym. Sci.*, 2003, **161**, 157–193.
32 B. C. van der Wiel, R. M. Williams and C. A. van Walree, *Org. Biomol. Chem.*, 2004, **2**, 3432–3433.
33 C. A. van Walree, V. E. M. Kaats-Richters, S. J. Veen, B. Wieczorek, J. H. van der Wiel and B. C. van der Wiel, *Eur. J. Org. Chem.*, 2004, 3046–3056.
34 J. March, *Advanced Organic Chemistry*, Wiley, New York, 4th edn, 1992.
35 M. Sundermeier, S. Mutyala, A. Zapf, A. Spanneberg and M. Beller, *J. Organomet. Chem.*, 2003, **684**, 50–55.
36 R. M. Williams, *Photochem. Photobiol. Sci.*, 2010, **9**, 1018–1026.
37 M. Lutz, A. L. Spek, B. C. van der Wiel and C. A. van Walree, *Acta Crystallogr., Sect. C: Cryst. Struct. Commun.*, 2005, **61**, o300–o302.
38 C. A. van Walree, B. C. van der Wiel, L. W. Jenneskens, M. Lutz, A. L. Spek, R. W. A. Havenith and J. H. van Lenthe, *Eur. J. Org. Chem.*, 2007, 4746–4751.
39 P. A. Limacher and H. P. Lüthi, *J. Phys. Chem. A*, 2008, **112**, 2913–2919.
40 M. Klokkenburg, M. Lutz, A. L. Spek, J. H. van der Maas and C. A. van Walree, *Chem.–Eur. J.*, 2003, **9**, 3544–3554.
41 N. N. P. Moonen and F. Diederich, *Org. Biomol. Chem.*, 2004, **2**, 2263–2265.
42 C. A. Van Walree, B. C. Van der Wiel and J. H. Van Lenthe, *Chem. Phys. Lett.*, 2012, **528**, 29–33.
43 C. A. van Walree, M. R. Roest, W. Schuddeboom, L. W. Jenneskens, J. W. Verhoeven, J. M. Warman, H. Kooijman and A. L. Spek, *J. Am. Chem. Soc.*, 1996, **118**, 8395–8407.
44 E. Lippert, *Z. Elektrochem.*, 1957, **61**, 962.
45 Note that in our earlier study (ref. 32) when no information on the ground state dipole moment was available, a slightly different expression was used.
46 Data were taken from: C. Reichardt, *Solvents and Solvent Effects in Organic Chemistry*, VCH, Weinheim, 2nd edn, 1988.
47 F. C. de Schryver, N. Boens and J. Put, *Adv. Photochem.*, 1977, **10**, 359–465.

48 J. W. Verhoeven, *Pure Appl. Chem.*, 1990, **62**, 1585–1596.
49 F. J. Hoogesteger, C. A. van Walree, L. W. Jenneskens, M. R. Roest, J. W. Verhoeven, W. Schuddeboom, J. J. Piet and J. M. Warman, *Chem.–Eur. J.*, 2000, **6**, 2948–2959.
50 W. D. Oosterbaan, C. Koper, T. W. Braam, F. J. Hoogesteger, J. J. Piet, B. A. J. Jansen, C. A. van Walree, H. J. van Ramesdonk, M. Goes, J. W. Verhoeven, W. Schuddeboom, J. M. Warman and L. W. Jenneskens, *J. Phys. Chem. A*, 2003, **107**, 3612–3624.
51 As documented before (ref. 33), the cavity radius of **DA1** was estimated by comparison with related compounds. The radius of **DA2** is assumed to be 0.2 Å larger.
52 R. A. Marcus, *J. Phys. Chem.*, 1989, **93**, 3078–3086.
53 J. Cortés, H. Heitele and J. Jortner, *J. Phys. Chem.*, 1994, **98**, 2527–2536.
54 The peak potentials are given here. Due to the irreversible nature of the reduction process of **DA1** and **DA2** the half wave potentials can only be approached. Since we are primarily interested in the differences between **DA1** and **DA2**, the peak potentials suffice.
55 I. R. Gould, D. Noukakis, L. Gomez-Jahn, R. H. Young, J. L. Goodman and S. Farid, *Chem. Phys.*, 1993, **176**, 439–456.
56 R. J. Cave and M. D. Newton, *Chem. Phys. Lett.*, 1996, **249**, 15–19.
57 A. M. Oliver, M. N. Paddon-Row, J. Kroon and J. W. Verhoeven, *Chem. Phys. Lett.*, 1992, **191**, 371–377.
58 I. R. Gould, R. H. Young, L. J. Mueller, A. C. Albrecht and S. Farid, *J. Am. Chem. Soc.*, 1994, **116**, 3147–3148.
59 M. Bixon, J. Jortner and J. W. Verhoeven, *J. Am. Chem. Soc.*, 1994, **116**, 7349–7355.
60 M. Rust, J. Lappe and R. J. Cave, *J. Phys. Chem. A*, 2002, **106**, 3930–3940.
61 M. N. Paddon-Row, M. J. Shephard and K. D. Jordan, *J. Phys. Chem.*, 1993, **97**, 1743–1745.
62 R. W. A. Havenith, C. A. van Walree, A. W. Marsman, J. H. van Lenthe and L. W. Jenneskens, *Phys. Chem. Chem. Phys.*, 2007, **9**, 1312–1317.
63 The similarity of a cross-conjugated C═C bridge and a bridge consisting of a single sp^3 hybridized atom has recently been described: R. Emanuelsson, A. Wallner, E. A. M. Ng, J. R. Smith, D. Nauroozi, S. Ott and H. Ottoson, *Angew. Chem., Int. Ed.*, 2013, **52**, 983–987.
64 D. F. Eaton, *Pure Appl. Chem.*, 1988, **60**, 1107–1114.
65 X. Y. Lauteslager, I. H. M. van Stokkum, H. J. van Ramesdonk, D. Bebelaar, J. Fraanje, K. Goubitz, H. Schenk, A. M. Brouwer and J. W. Verhoeven, *Eur. J. Org. Chem.*, 2001, 3105–3118.
66 M. J. Frisch, *et al.*, *Gaussian, 09, Revision. 01*, Gaussian Inc., Wallingford, CT, 2010.

